Fluorination of flax fibers for improving the interfacial compatibility of eco-composites

Olivier Téraube, Jean-Charles Agopian, Monica Francesca Pucci,
Pierre-Jacques Liotier, Samar Hajjar-Garreau, Nicolas Batisse, Karine
Charlet, Marc Dubois

Fluorination of flax fibers for improving the interfacial compatibility of eco-composites

Olivier Téraube [a,b,*], Jean-Charles Agopian [a,b], Monica Francesca Pucci [c], Pierre-Jacques Liotier [d], Samar Hajjar-Garreau [e], Nicolas Batisse [a], Karine Charlet [b], Marc Dubois [a]

[a] Université Clermont Auvergne, Clermont Auvergne INP, ICCF, BP 10448, 63000 Clermont-Ferrand, France
[b] Université Clermont Auvergne, Clermont Auvergne INP, Institut Pascal, BP 10448, 63000 Clermont-Ferrand, France
[c] LMGC, IMT Mines Ales, Univ Montpellier, CNRS, Ales, France
[d] Polymers Composites and Hybrids (PCH), IMT Mines Ales, Ales, France
[e] Institut de Science des Matériaux de Mulhouse, CNRS-UMR 7361, Université de Haute-Alsace, 68057 Mulhouse, France

ABSTRACT

Because of their specific properties, vegetal fibers are increasingly used as sustainable polymer reinforcements for eco-composites. Nevertheless, their polar character hinders them from being used more frequently at in-dustrial scale due to their incompatibility with mostly dispersive polymers (the cheapest and most common ones). In this study, direct fluorination treatment was carried out to covalently graft fluorine atom at the outmost surface of flax fibers. Such a grafting has been proved by FT-IR, ^{19}F NMR and XPS spectroscopies, and these characterizations allowed to understand chemical change due to the treatment. This chemical modification induced an augmentation of the dispersive character of flax fibers, by significantly lowering the polar component of surface energy without significant change of the dispersive component. Young's modulus was also maintained. Thereby, treated fibers become perfectly compatible with hydrophobic polymer, and an improvement in the mechanical performance of the resulting composite is expected according to the literature.

1. Introduction

Vegetable fibers are increasingly used to substitute glass fibers as polymer reinforcement for eco-composites manufacturing. Indeed, in addition to the fact that vegetal fibers and glass fibers present similar specific properties, the use of the former allows bio-based and local resources to be valorized while lightening the overall weight and reducing the cost of composites [1–8]. Therefore, all these advantages allow them to be more and more used in the transportation industry (aeronautics, automotive, etc.). Their use is expected to increase due to current environmental issues and the emerging context of the bio-economy aimed at continuing economic growth while preserving the environment and earth resources [1,4,8].

Mechanical performances of composite materials are mainly related to the quality of the fiber/matrix interface. However, if flax fibers are considered as one of the best natural reinforcement for polymer matrix [9] because of their very good mechanical properties [10–12], their sensitivity to water sorption makes them difficult to use as is. Indeed, cellulose, lignin, and hemicelluloses that compose lignocellulosic materials have a high number of hydroxyl and carboxyl groups in their chemical structure. Their polarity is relatively high, i.e. γ_s^p of 26,0 mN/m whereas a dispersive component γ_s^d of 34 mN/m is typically measured [13], that raises several issues in the use of these fibers as polymer reinforcement. On the one hand, this character makes them sensitive to water and moisture sorption, questioning the viability of vegetal fiber composite in humid environment. Indeed, swelling and shrinkage are caused by water absorption and desorption, and this change in fiber morphology may lead to cracks in the composite structure [14]. On the other hand, the high polarity of flax fibers induce a lack of compatibility with hydrophobic resin (the most common and cheapest ones), that makes the fibers difficult to be wetted by these matrix [15–17]. This incompatibility results in a poor effective adhesion, partly due to micro-porosities, between fibers and matrix that would greatly weaken the mechanical performance of these eco-composites [6,14,18,19]. Most of the time, people are talking about the hydrophilic character of the fibers which makes them incompatible with hydrophobic polymers. These terms, "hydrophilic" and "hydrophobic", are often confusing because they are only related to water interaction and do not allow to perfectly

---

* Corresponding author at: Université Clermont Auvergne, Clermont Auvergne INP, ICCF, BP 10448, 63000 Clermont-Ferrand, France.
E-mail address: olivier.teraube@uca.fr (O. Téraube).

and rigorously describe the physical-chemical interactions that take place at the fiber/matrix interface within the composite. Therefore, the notions of polarity and dispersivity will be privileged in this paper (hydrophilicity being mostly related to a high polarity, while hydrophobicity is related to a low polarity).

Thereby, in order to achieve the optimal mechanical performance of these composites, it is necessary to compatibilize these fibers with the polymer matrix. Over the time, several chemical and/or physical methods were developed with this aim, e.g. thermal treatment [20–22], electric discharge [23,24], chemical treatment (acetylation, MAPP treatment, mercerization, etc.) [25–31] or sizing deposition [32,33]. These treatments allowed to decrease the polarity of the lignocellulosic fibers, thus reducing the presence of cavities at the fiber/polymer interface. In addition, Liotier et al. [34] have proved that even if treatments may make fibers more brittle, improvement of the wettability of fibers by the matrix allows the improvement of the overall mechanical behavior of manufactured composites. However, these treatments are unfortunately costly, both time and energy consuming, and/or harmful to the environment and people by using toxic solvents or chemicals. This induces in all cases an increase of the carbon dioxide footprint of the composite manufacturing processes, which is inconsistent with the principle of "eco-composite" aiming to reduce as much as possible the environmental impact of these materials.

Nowadays, many researcher are looking to develop novel "green" methods to achieve this compatibilization without impacting the environment [35–43]. However, these approaches are generally difficult to scale up to an industrial scale, requiring additional investments and/or the development of new technologies.

Direct fluorination i.e. the treatment of substrate with pure fluorine or fluorine diluted with an inert gas (nitrogen, helium etc.), is frequently used at the industrial scale in order to enhance various properties of polymeric materials [44]. In mild conditions, this chemical treatment acts only on a thin part of the substrate (~0.01–10 μm on the surface) without a change the bulk, allowing the initial properties of raw materials to be preserved [44–47]. Among the different properties brought with this fluorinated layer such as the reduction of the permeability to hydrocarbons and other compounds, the enhancement of friction properties, the improvement of the chemical resistance, etc. [44,46,48], direct fluorination allows to reduce the polar character of materials [45,46,49–52]. Moreover, as a gas/solid reaction, fluorination is performed without using toxic solvent in a closed reactor without release of any toxic substance in the atmosphere, and the reaction could be spontaneously performed at room temperature; so that this treatment exhibits a very low environmental footprint. In addition, the method is fast, without any human contact with the reactant, reproducible, and thus presents all the advantages required for an eco-responsible industrial way to make vegetable fibers less polar.

It is in this context that we propose to use a direct fluorination treatment to make flax fibers more dispersive in a "eco-friendly" way. This study investigates therefore the effect of a treatment under molecular fluorine (F_2) on flax fibers. The strategy consists in covalently graft fluorine atoms on the outmost surface of flax fibers in order to reduce the polar character of the latter without modification of their bulk characteristics. These assumptions will be confirmed by complementary characterization techniques et different level, surface (XPS, tensiometry) and bulk (NMR, mechanical tests).

In addition, torrefaction treatment is frequently used at industrial scale to reduce the polar character of vegetal fibers by destroying hemicelluloses, the most polar component of lignocellulosic materials. It consists in a pyrolysis between 200 and 300 °C in the absence of oxygen during a "short" duration [53,54]. Because it has been proven that this treatment improves the mechanical performance of flax-based composites by reducing the polarity of these fibers [34], a comparison between both treatment will be realized.

2. Experimental

2.1. Fluorination

Fluorination of flax fibers was performed inside a passivated nickel reactor (covered with NiF_2) in static conditions. The sample were placed into a vacuum chamber. When vacuum was achieved (10^{-3} bar), the chamber was filled with F_2/N_2 (1/4 Vol./Vol.) mixture, followed by the evacuation of fluorine after the treatment. Flax fibers were pieces of FlaxTape™, purchased from Eco-Technilin, whose dimensions were 50 × 4 cm^2. Chemical composition of dried fibers have been measured using ADF-NDF-ADL method, according to [55]. Four measurements were performed, and results are presented in Table 1.

The reactive gas consists of a mixture of pure fluorine, purchased from Solvay Fluor (<0.1 vol% of admixtures, mainly oxygen), and pure Nitrogen (99,999% purity). Before each reaction, fibers were outgassed during 2 h under primary vacuum (10^{-3} mbar) at 80 °C. Then, the reactor was flushed for 1 h with nitrogen gas to remove all traces of air and moisture. Then, one strip of fibers was placed into the reactor, during 1 h under primary vacuum (10^{-3} mbar) at room temperature. At this moment, the pump was switch off, and the reactor is then under a pressure of 10^{-3} mbar. 200 mbar of N_2, then 300 mbar of F_2 and finally 500 mbar of N_2 (at a high flow rate in order to generate flow into the reactor) were injected. Reactions were performed at room temperature for 5 min, 10 min, 20 min and 60 min. Once the fluorination time was over, reactor was flushed with pure nitrogen gas for 1 h to both stop the reaction and remove the traces of unreacted F_2, HF, CF_4, and C_2F_6 (hose gases were removed by a soda lime trap). Finally, the fibers were once again outgassed for 1 h under primary vacuum (10^{-3} mbar) at 80 °C for the completion of removal of all fluorine-based gases from the sample surface.

In addition to previous samples, another one, named "over-fluorinated" has been prepared (Fig. 1b). The latter has been treated with a very large amount of fluorine (not quantifiable), by remaining inside the reactor during maintenance session. The duration is higher than 24 h and the resulting material is representative of the complete decomposition and perfluorination of the fibers.

2.2. Torrefaction

Torrefaction of flax fibers was carried out according to the optimized treatment described by Berthet et al. in order to improve fiber/matrix adhesion in a biocomposite [22]. Thereby the following sequence was performed:

- Step 1: Drying at 110 °C for 1 h, under a N_2 flow rate (60 mL/min).
- Step 2: Heating ad 230 °C for 45 min, under a N_2 flow rate (60 mL/min).

2.3. Characterization

FTIR experiments were carried out with a Nicolet 6700 FT-IR (Thermo Scientific) spectrometer in ATR mode. For each spectrum, 32 scans with 4 cm^{-1} resolutions were collected between 4000 and 524 cm^{-1}.

^{19}F solid state NMR spectra were recorded using a 300 MHz Bruker Avance spectrometer. A magic-angle spinning (MAS) probe operating

Table 1
Chemical composition of dried raw fibers.

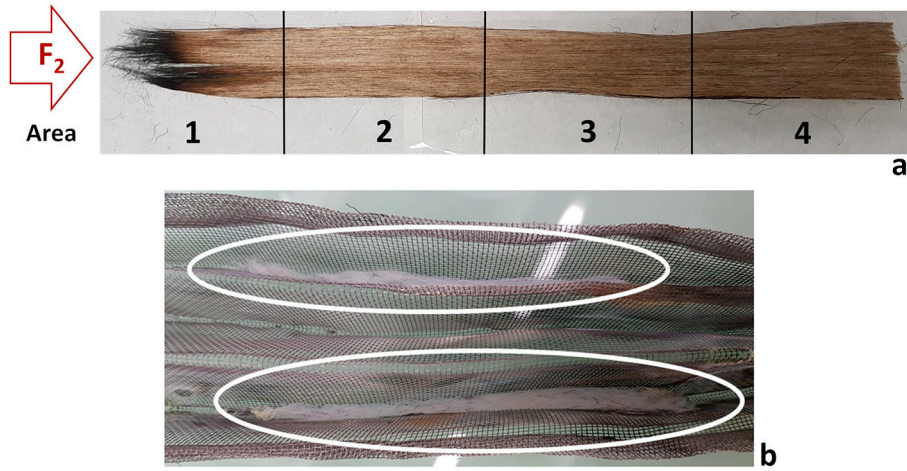|	Experimental (%)	Theoretical (%) [3,56]
Lignin	2.4 ± 0.4	2–3
Cellulose	75.8 ± 3.6	60–81
Hemicelluloses	13.6 ± 6.8	14–21
Extractives	8.2 ± 2.9	<10

Fig. 1. (a) a representative example of the fluorinated samples; zone 1 is the closest from the F₂ gas injection" and (b) Overfluorinated" sample.

with 2.5 mm rotors was used allowing a 30 kHz spinning rate. A simple sequence was used with a single $\pi/2$ pulse with a duration of 4.0 μs. ^{19}F chemical shifts were externally referenced to CF₃COOH and then referenced to CFCl₃ ($\delta_{CF_3COOH}=-76.6$ ppm vs δ_{CFCl_3}).

XPS measurements were performed with a VG Scienta-SES 2002 hemispheric analyzer, a monochromatized XPS source (AlK$_\alpha$: h$\nu =$ 1486.6 eV) and an electron gun for charge effect compensation.

Spectra were recorded using pass energy of 100 eV for the spectra in high resolution and 500 eV for the general spectrum (wide scan). The analysis area was about 4x6mm².

Peaks were fitting by Gaussian-Lorentzian functions using the XPS-CASA software (casaXPS software 2.3.18 Ltd., Teignmouth, UK) after having substrated a Shirley-type background. The quantity and the atomic percentage of the elements present on the surface were determined by integrating peak areas of each component considering the transmission function of the spectrometer, the effective cross section and the mean free path of each atom.

To calculate this atomic percentage, C1s, O1s and F1s lines were taken into account.

Surface modifications of samples were also investigated using scanning electron microscopy (SEM). During those investigations, the energy of the electron beam was 3KeV and for each sample, pictures were captured at 2000× of magnification.

Surface roughness of sample was measured by atomic force microscopy (AFM). Experiments were carried out using a Bruker Innova® Atomic Force Microscope equipped with a RTESPA-300 8 nm radius silicone probe. For each sample, a surface of 2 μm × 2 μm, in tapping mode with resonant frequency of 0.5 Hz.

In order to estimate the change in the surface energy due to treatments, the determination of the contact angle between fibers and different liquids is necessary. To measure this contact angle, the most common method is the "sessile drop" technique [57]. However, this technique cannot be employed with fibers and fabrics, because of their shape and texture that induces a fakir effect distorting the measurements. Thereby, several methods have been developed along time in order to perform this measurement on single fibers [58–61]. Nevertheless, among them, the tensiometric one seems the most convenient. As described by Qiu et al. [59], it is based on the use of a Wilhelmy balance and the Wilhelmy relationship (1)

$$F = \gamma_l \quad pcos\theta \tag{1}$$

where F is the capillary force (mN), p (m) the wetted length, θ (°) the contact angle and γ_l (mN/m) the surface tension of the liquid.

The procedure carried out in this paper was the same than the one described in Pucci et al. [13].

Measurements were performed using a Krüss K100SF tensiometer. To measure the contact angle with a given liquid, a single fiber is first extracted from the strips of fibers. This one was placed in a clamp within the tensiometer and placed as close as possible to a crystallizer filled with n-hexane (purchased at Sigma-Aldrich, ReagentPlus 99%), without touching it. This crystallizer advanced at a speed of 1 mm/min and came in contact with the fiber. Then it went up to a depth immersion of 5 mm, the tensiometer allowing to measure the capillary force exerted by the n-hexane on the fiber. Since the n-hexane has a totally wetting behavior, we considered that the wetting angle between the fiber and the latter is 0°, and therefore that the eq. (1) can be written as follows (2), allowing to determine the perimeter of the fiber:

$$F = \gamma_l \quad p \tag{2}$$

In a second step, the same fiber was placed as close as possible to the test liquid (water or diiodomethane). The vessel was then rised of 5 mm at a speed of 1 mm/min (advancing). Once realized, it remains at this position during 60s (static) and finally come back to its initial position (receding). To measure the static contact angle, the first point after the 60s of immobility was used.

Static contact angle was therefore calculated using the Wilhelmy eq. (1), and the wetted length previously calculated with the n-hexane experiment.

To determine the polar and the dispersive component of the surface tension of fibers, the Owens-Wendt method was considered [62]. This theory is based on the eq. (3) that allows to determine the dispersive and polar components of the fiber surface energy (γ_s^d and γ_s^p).

$$\frac{\gamma_l(1 + cos(\theta))}{2\sqrt{\gamma_l^d}} = \sqrt{\gamma_s^p}\left(\frac{\sqrt{\gamma_l^p}}{\sqrt{\gamma_l^d}}\right) + \sqrt{\gamma_s^d} \tag{3}$$

Because eq. (3) has two unknown parameters (γ_s^d and γ_s^p), at least two contact angle measurements with two liquids are mandatory. In this study, water and diiodomethane (purchased from AlfaAesar, 99%, stab. with copper) were used and their respective polar and dispersive components are available in Table 2. Then, because eq. (3) is of the form Y = aX+B, by plotting $\gamma_l(1 + cos(\theta))\big/2\sqrt{\gamma_l^d}$ (y axis) versus $\sqrt{\gamma_l^p}\big/\sqrt{\gamma_l^d}$ (x axis) for each liquid, the slope and the y-intercept of the linear fit are the

Table 2
Surface energy and components of tests liquid (according to [63]).

Liquid	γ_l (mN/m)	γ_l^d (mN/m)	γ_l^p (mN/m)
Eau	72.8	21.8	51.0
Diiodométhane	50.8	50.8	0.0
n-Hexane	18.4	18.4	0.0

square root of fiber polar and dispersive components, respectively. For each sample, at least 5 measurements were performed with both test liquids, and the mean value of θ was used to plot data. The uncertainties on surface energy components were measured using the maximum and minimum slopes techniques.

DVS (Dynamic Vapor Sorption) analysis allows to continuously measure the water absorption uptake of the samples and to see if the applied treatments have modified this property. However, traditional equipment requires a significant mass of materials in a restricted space, which makes it difficult to be performed on fibers.

Thereby, to still performed this measurement, we transformed a MetlerToledo ME104 balance into an equivalent DVS measuring equipment. To realize this, 4 crystallizers were filled with saturated solution of NaBr. Indeed, according to the ISO 483:2005 standard [64], it was possible to fix the percentage of relative humidity (RH%) in an enclosed space. More precisely, NaBr fixed the RH% at 59% at 20 °C. Therefore, by tightly closing the dust cover on top of the weighing module, it was possible to fix the RH% at 59 ± 2% (depending on thermal condition inside the room). Finally, the balance was, via a RS232 cable, linked to a computer which, using RSweight software, allowed the acquisition of the recorded mass.

To carry out the experimentations, sample (around 0.5 g of fiber) were dried at 80 °C under vacuum (10^{-3} mBar) for 24 h. Then, the RH% was checked before the beginning of the experiment using a fisherbrand Traceable®Hygrometer, to ensure that the RH% was at 59 ± 2%. If the previous condition is met, dry fibers were placed into a watch glass place into the balance. The cover was tightly closed, and the acquisition launched for at least 1000 min. Once the time was over, RH% was checked again.

X-ray diffraction (XRD) analyses of raw and treated flax fibers were carried out to identify change in the chemical structure of cellulose as the loss of semi-crystallinity. Sample were prepared by positioning fibers on a "zero diffraction plate" made with monocrystalline silicon, to avoid any signal from the support plate. Diffractograms were recorded on a PANalytical X′ Pert Pro Powder Diffractometer equipped with a Cu anticathode ($\lambda_{K\alpha1} = 1.540598$ Å, $\lambda_{K\alpha2} = 1.544426$ Å) and an X′celerator RTMS detector. The acceleration voltage filament current was fixed at 40 kV and 30 mA respectively. Diffractograms were recorded between 5° and 55° in 2θ with a step size of 0.0668° at a scanning rate of 5°/min. During the acquisition, a sample rotation of 1°/s was applied, in order to eliminate fiber orientation effects.

In order to identify potential release of fluorine gas during flax fibers combustion, thermogravimetric analysis coupled with mass spectrometry (TGA/MS) was performed under a continuous flow of 99,999% v/v He gas. The set up was an STA Netzsch Jupiter F3 analyzer with a heating ramp of 10 K min^{-1}. Gas releases from the sample during the temperature rise were analyzed with an online quadrupole mass spectrometer Netzsch QMS 403 Aeolos Quadro.

The mechanical properties (Young's modulus (E), Ultimate tensile strength (σ_m) and maximal elongation percentage (%ε)) were investigated via tensile tests of raw and fluorinated flax fibers. For each sample, at least 50 single fibers were glued on different paper frames, according to [65]. Their diameter was estimated from the average of 3 microscopes measurements (1000× of magnification). Then, tensile test was carried out using an Instron 5543 device equipped with a 50 N load cell. During experimentations, the gauge length was 10 mm and the crosshead displacement rate was 1 mm/min, up to rupture. Finally, the different properties (E, σ_m, %ε) were calculated according to the C standard [66].

3. Results and discussion

3.1. Homogeneous fluorine grafting

According to both the reactivity of F_2 gas and the tubular geometry of the reactor with a gas injection on one side, the first parameter which must be studied is the homogeneity of the treatment. In the area 1,

which is closer to the fluorine injection, an inhomogeneity is present as seen by Fig. 1a with apparent burning. Thereby, ^{19}F NMR was performed on each area of each sample. In addition, to prove the covalent grafting of F atoms, results (Fig. 2) evidence the homogeneity. Indeed, for 5 and 10 min of fluorination, the line shapes are almost superimposed; nearly the same chemical modifications have been achieved on the surface of the flax fibers. The shorter the reaction duration, the more homogenous the fluorination. Nevertheless, it is possible to conclude that fluorination treatment is homogeneous at least on zone 2 and 3. Some difference may be observed on zone 1 and 4, but only after a long fluorination time (> 10 min). Consequently, for the other characterization, analyses were performed with samples located on area 2 or 3, and samples will be named FT-Xmin with X the fluorination duration in minutes.

3.1.1. Chemical composition in the fluorinated layer

In order to better understand the chemical changes of composition with the fluorination reaction, FT-IR and ^{19}F solid state NMR were performed. Deconvolution of IR spectra evidences the appearance of several carbon-fluorine vibration bands between 1000 and 1400 cm^{-1} on the IR spectra (wine color lines in Fig. 3), that, according to [67], correspond to the C—F stretching band. This unambiguously evidenced the creation of covalent C—F bonds.

Between 5 and 10 min of fluorination, contribution of C—F assigned bands increased, underlining that up to 10 min, the longer the treatment, the higher the amount of grafted fluorine. For 20 min treatment, this C—F contribution decreased compared to 10 min. This is related to the beginning of a degradation phenomenon. Indeed, as already observed for polymer and wood fluorination [48,68–71], when the time of fluorination process is too long, a disruption of the main carbon chain occurs and gaseous compounds (CF_4, C_2F_6, etc.) are released. Here, even if fluorine grafting increases, the intensity of the C—F bands decreases due to this degradation of the carbon skeleton. Moreover, the same area (1000–1400 cm^{-1}) also corresponds to C—H and C—O stretching bands which are typical of the natural fibers structure. Those latter groups are
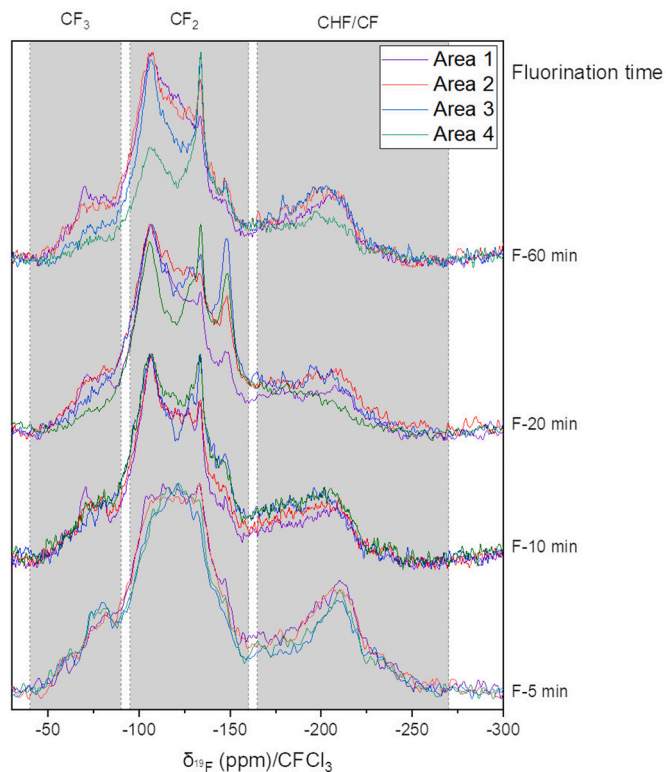

Fig. 2. Comparison of ^{19}F NMR spectra (solid state) recorded on every zone of every sample.
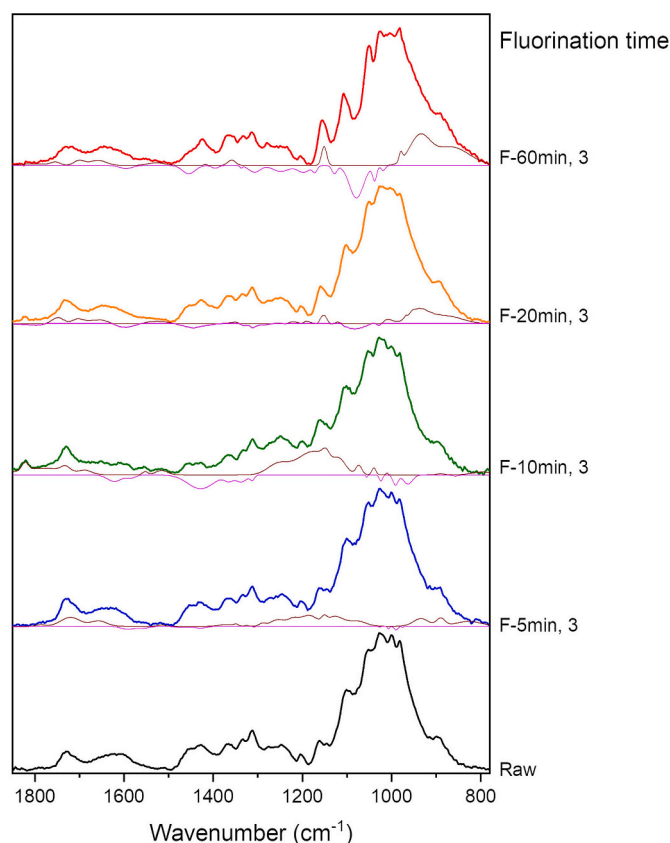
Fig. 3. FT-IR spectra of raw and fluorinated flax fibers. For fluorinated samples, the wine and pink lines, close to the horizontal line correspond respectively to the "positive" and "negative" spectrum contribution compared to the raw sample spectra. Raw spectrum is subtracted from that of the fluorinated fibers in order to make appear the "positive" and "negative" contribution by the difference between both spectra.

converted into CHF, CF_2 or CF_3 groups. Both samples after 20 min and 60 min of fluorination exhibit signs of degradation. Indeed, for 60 min duration, negative contributions appear evidencing that degradation has become preponderant compared to fluorine grafting.

To go deeper in the understanding of the chemical modifications which took place during the fluorination treatment, ^{19}F NMR experimentations were carried out and the data are presented in Fig. 4. Pouzet et al. [69] have previously showed that fluorination of lignocellulosic materials (such as flax) only affects lignin, which is basically an amorphous polymer. However, polymer fluorination mainly transforms CH_x groups into CF_3, CF_2 or CH_yF (y = 1 or 2) groups [48,72]. Chemical shifts of these three groups are respectively between $-40/-90$ ppm, $-100/-155$ ppm, $-160/-250$ ppm (highlighted with a grey background in Fig. 4). During this chemical reaction, fluorine reacts on double bonds and C—H bonds until perfluorination without disruption of the C—C skeleton: C—CF_2—C (or C—CF(—C)—C). However, if after this step, the reaction may go further through disruption of C—C bond and CF_3 groups are created because of the reaction of the dangling bonds (radicals) with F_2 [46,48,68].

Thereby, according to the line shape as the time of fluorination (Fig. 4), it increases; peaks becomes to be finer and finer and tend towards the NMR spectrum of the "overfluorinated" compound (considered as the ultimate step). The narrowness of lines for high fluorination rates is explained by the homogenization of the chemical structure in the fluorinated layer; the neighboring (e.g. CF_2—CFH—CF_2, CHF—CFH—CF_2, CHF—CFH—CHF, CH_2—CFH—CH_2...) is perfluorinated. As a consequence, the lines with the corresponding chemical shift dominate. It is important to note that the width of each line is
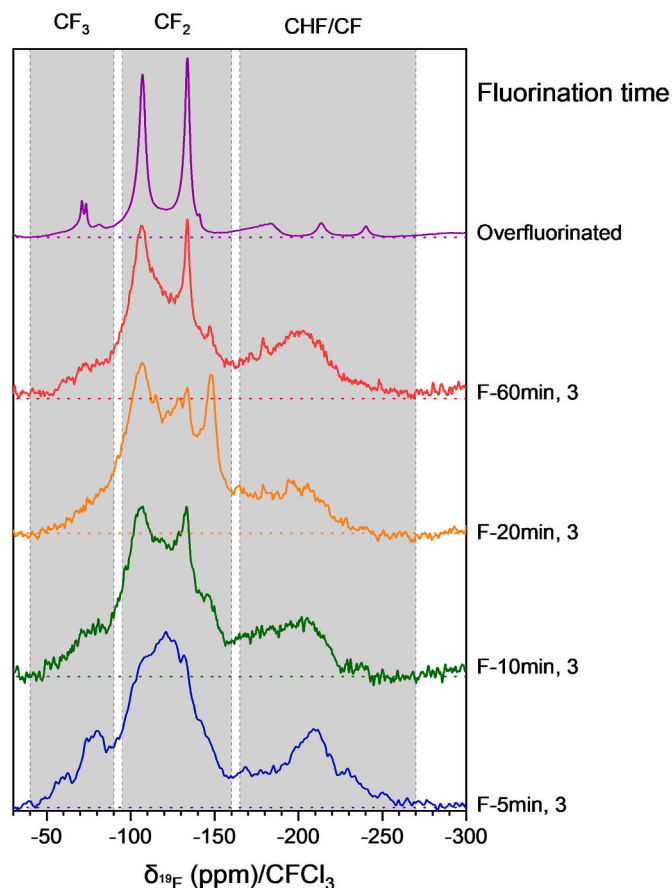
intrinsically broad because of ^{19}F—^{19}F homonuclear dipolar coupling. Therefore, with increasing treatment, a unique chemical structure tends to dominate as for the "overfluorinated" compound. Thereby, the identification of the chemical structure of this particular sample would allow to better understand the fluorination reaction mechanism of flax fibers. We paid attention on it although it consists in a decomposition residue.

First, the white color of the "overfluorinated" compound (Fig. 1b) reminds the color of fluorinated polymers (PTFE and PVDF) [73]; the greenish color is related to the presence of NiF_2 from the fluorination of

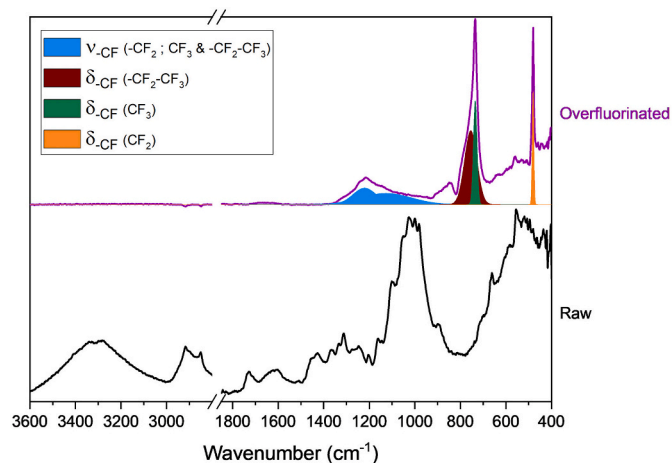**Fig. 4.** ^{19}F solid-state NMR spectra of fluorinated flax fibers.

Fig. 5. Comparison between FT-IR spectra of raw flax fibers and overfluorinated ones.

nickel boat. Then, Fig. 5 and Fig. 4 (at the "overfluorinated" label) display the comparison between FT-IR spectrums of raw flax fibers and "overfluorinated" ones, and the ^{19}F spectra of the "overfluorinated" compound, respectively. On the FT-IR spectra, we clearly notice the disappearance of the —OH band between 3000 and 3500 cm^{-1} ($\nu_{—OH}$) and the —CH bands between 2800 and 3000 cm^{-1} ($\nu_{—CH}$) evidences the total removal of both the hydroxyl and CH_x groups from the chemical structure of flax fibers. This phenomenon is also visible at lower wavenumbers (400–1900 cm^{-1}) with the disappearance of the majority of the vibration bands which are assigned to C—O, C=C, C—H and O—H [67]. In addition, new bands appear at 1350–1000 cm^{-1}, 800–650 cm^{-1} and 460–500 cm^{-1} and are assigned respectively to $\nu_{—C—F}$ for —CF$_2$, —CF$_3$ and —CF$_2$—CF$_3$ groups, $\delta_{—C—F}$ for —CF$_3$ and —CF$_2$—CF$_3$ and $\delta_{—C—F}$ for—CF$_2$ according to [67]. Thereby, after this over-fluorination, only fluorocarbon groups (CF$_2$ and CF$_3$ mainly) constitute the chemical structure which is close to the one of polytetrafluoroethylene (PTFE). The change of the ^{19}F NMR line shapes can be further discussed according to this observation.

According to Vega et al. [73] CH$_2$ of PTFE have two different chemical shifts depending if there are in the semi-crystalline or in the amorphous part. Later, Katoh et al. [74], based on works previously mentioned, have succeed to identify the chemical shift of an irradiated PTFE and their works were then completed by Fuchs & Scheler [75] and by Dargaville et al. [76]. The chemical groups identified here correspond to those identified by FT-IR in our compound, and whose NMR spectra are similar to ours. Thereby, assignments presented in Table 3 have been done and those ones are applicable to our fluorinated compounds. After 5 min of fluorination we notice that the intensities of −107 ppm, −120 ppm and −130 ppm peaks are similar, indicating that their corresponding chemical groups (Table 3) are in equivalent quantities (intensity can be directly compared because of the fact that those 3 groups are all related to CF$_2$ groups, and therefore it is not necessary to apply a weighting). Then, with the increase of the fluorination time, −120 ppm lines fades away in front of the two other ones, evidencing that increasing fluorination duration lowers the crystallinity of the fluorinated layer. By comparing "fluorinated" "overfluorinated" samples, we also notice that with the overfluorination treatment, CHF lines (chemical shifts below −190 ppm [49]) are completely removed, and only the lines related to CF groups linked with three other carbons (around -190 ppm [74–76]) remain. Indeed, those specific carbons are

saturated with one fluorine atom in the perfluorinated state. Finally, it is important to note that the fluorination treatment does not produce high content of CF$_3$ groups, even for 60 min and under over-fluorination conditions; those groups are continuously created and decomposed into CF$_4$ or C$_2$F$_6$.

3.1.2. Surface chemical modifications

Chemical changes were also studied by XPS focusing on the outmost surface of sample. XPS spectra of raw and fluorinated flaw fibers were investigated via C1s deconvolution (Fig. 6). The spectra of raw flax fibers exhibit 4 contributions at: 284.9, 286.6, 288 and 289 eV. The first peak was attributed to both Csp^2 of lignin aromatic cycles and Csp^3 (C—C/C—H) which composed lignin, cellulose and hemicelluloses, and thus. Second one is related to carbon bonded with an oxygen through a single bound (C—OH, C—O—C or phenyl—OH). The third one is associated to carbonyl carbon (C=O). Finally, the last one corresponds to Csp^3 of ester and carboxyl groups [77–80]. In addition to C1s deconvolution, other peaks are available in supporting information.

After direct fluorination, the peak at 688 eV that appeared on the XPS survey is an additional proof of fluorine grafting onto the fiber surface [81]. Thanks to the general survey, it is possible to quantify the atomic percentage (Table 4). Initially, flax fibers are mainly composed of carbon and oxygen. When fibers undergo a fluorination treatment, fluorine is covalently grafted at the outmost surface of fibers with a F/C atomic ratio of 0.39 after 5 min fluorination and up to 0.82 for 60 min fluorination. Meanwhile, O/C ratio also grows from 0.14 to 0.28 at 20 min of fluorination and it decreases at 0.21 for 60 min of fluorination. This phenomenon was already observed on polybenzoxazole (PBO) fibers fluorination by Luo et al. [81]: the surface was more and more loaded in oxygen when the fluorination duration increases. Dangling bonds formed by fluorination are not fully saturated with F$_2$ and the remaining radicals react with oxygen and moisture during the exposure to air after the completion of the process.

In addition, 7 new contributions appeared on the C1s spectra. The first one at 286.6 eV (same position than C—O peak) is related to C positioned alpha to CF$_x$ groups. Then, 2 peaks at 287.2 and 288.8 are both assigned to —CF group as CH$_x$—CF— CH$_x$ and CF$_x$—CF— CF$_x$. Finally, the 291.0 peak is attributed to CF$_2$ groups and the 293.6 one is associated to CF$_3$ [77–80,82–84]. In addition to carbon peaks in the same region, two components appear with the fluorination treatment, at

Table 3
Assignments of peaks in overfluorinated compound, according to [74–76].

Group	Theorical chemical shift	Experimental chemical shift	Assignment	
-CF$_3$	−69 ppm (crystalline) −72 ppm (amorphous)	−70 ppm −74 ppm	$\begin{array}{ccc} F_2 & F & F_2 \\ —C & –C—C & — \\ & \vert & \\ & CF_3 & \end{array}$	
	−84 ppm	−81 ppm	$\begin{array}{c} F_2 \\ R_F—C –CF_3 \end{array}$	
CF$_2$	−108 ppm/−110 ppm	−107 ppm	$\begin{array}{ccc} F_2 & F & F_2 \\ —C & –C—C & — \\ F_2C & & \\ \vert & & \end{array}$	$\begin{array}{ccc} F_2 & F & F_2 \\ —C & –C—C & — \\ & \vert & \\ & CF_3 & \end{array}$
	−120 ppm	−120 ppm	$\begin{array}{c} F_2 \\ R_F—C –R'_F \end{array}$ amorphous	
	−124 ppm	−130 ppm	$\begin{array}{c} F_2 \\ R_F—C –R'_F \end{array}$ crystalline	
	−128 ppm	−140 ppm	$\begin{array}{c} F_2 \\ R_F—C –CF_3 \end{array}$	
	−154 ppm	−148 ppm	$\begin{array}{c} \diagdown \quad \diagup \\ CF\text{-}CF \\ \diagup \quad \diagdown \end{array}$	
CF	−190 ppm	−185 ppm	$\begin{array}{c} F \\ —C— \\ \vert \end{array}$	

Fig. 6. C1s XPS spectra of flaw fibers (a) raw, (b) F-5 min, (c) F-10 min, (d) F-20 min, (e) F-60 min.

Legend (Fig. 6):
- C-C ; C-H ; C=C
- CF_x-$\underline{C}$-CF_x and C-OR
- O-C=O
- C-$\underline{CF}$-C
- CF_x-$\underline{CF}$-CF_x and C=O
- CF_2
- CF_3
- $K_{2p_{3/2}}$
- $K_{2p_{1/2}}$

Table 4

XPS surface atomic composition of raw and fluorinated flax fibers.

	Atomic percent (%)			Atomic ratio	
	C	O	F	O/C	F/C
Raw	87.9	12.1	/	0.14	0
F-5 min	62.1	12.2	24.2	0.19	0.38
F-10 min	61.6	11.8	25.2	0.19	0.40
F-20 min	52.3	14.5	32.3	0.27	0.61
F-60 min	48.7	10.3	40.3	0.21	0.82

Table 5

Percentage of carbon-based groups from XPS C1s spectra of raw and fluorinated flax fibers.

	Group percent (%)			
	CH/CC	CF	CF_2	CF_3
Raw	73,9	/	/	/
F-5 min	37.7	10.9	4.5	0.3
F-10 min	27.7	13.4	7.1	0.6
F-20 min	16.7	14.8	10.5	1.1
F-60 min	4.8	20.1	11.0	1.2

294.0 and 296.7 eV, their binding energies are too high to correspond to any C—F bond and attributed to the $K_{2p2/3}$ and $K_{2p1/2}$ with a spin-orbit coupling of 2.8, respectively [85]. This shows the presence of potassium (K) at the fibers surface after the fluorination treatment. If the exact reason for this is not known, we assume that it was already present in the core of the fibers. Indeed, it is well known that flax steam contain potassium in their structure [86,87], in the same way as the other parts of the flax plant (leaf, seed, etc.); the quantity depends on the year, the place, and the weather conditions in which the plants have grown [86–90]. Subsequently, the combined action of the thermal pre-treatment and the primary vacuum (10^{-3} mbar) would have caused this element to migrate to the fibers surface, transported by the desorbed water. The high affinity of potassium for F (to form KF) may also serve as a driving force for this potassium diffusion.

Fig. 6 displays the evolution of carbon-based group C1s peak, and Table 5 quantifies this evolution. All fluorinated samples (Fig. 6 b–e) exhibit the four peaks of CF_x groups and the higher the fluorination duration, the higher the percentage of CF_x groups. Moreover, we also notice that the decrease of the contribution of the peak at 284.9 eV is in good accordance with a perfluorination process (see Scheme SI1), as already observed on both polymer and wood fluorination [45,48,49,72,69,91].

As a partial conclusion, fluorine reacts on lignin (as demonstrated by Pouzet et al. [69]) and forms a fluorinated layer at the fiber outmost surface. The longer the treatment, the more the C—H and C—OH are converted to CF_x groups. However, if the fluorination is prolongated (from 20 min in our case), degradation occurred.

3.2. Impact of fluorination

3.2.1. Modification of the surface tension

Fluorine grafting at the outmost surface of materials is known to modify the surface energy of the latters, by reducing its polar component (γ_s^p). In order to identify and quantify modifications resulting from the fluorination treatment on fibers, wetting tests by tensiometric method were carried out. Fig. 7a summarizes the evolution of polar (γ_s^p), dispersive (γ_s^d) and total (γ_s) surface energy of fluorinated flax fibers. We first notice that the polar component is significantly modified by the fluorination treatment and a multi-scale characterization is needed to understand the observed behavior.

The evolution of the polar component could be explained by the fact that for 5 min fluorination, fluorine was grafted on very few sites on the surface of the fibers, as seen on the XPS analysis (Fig. 6, Table 4 and
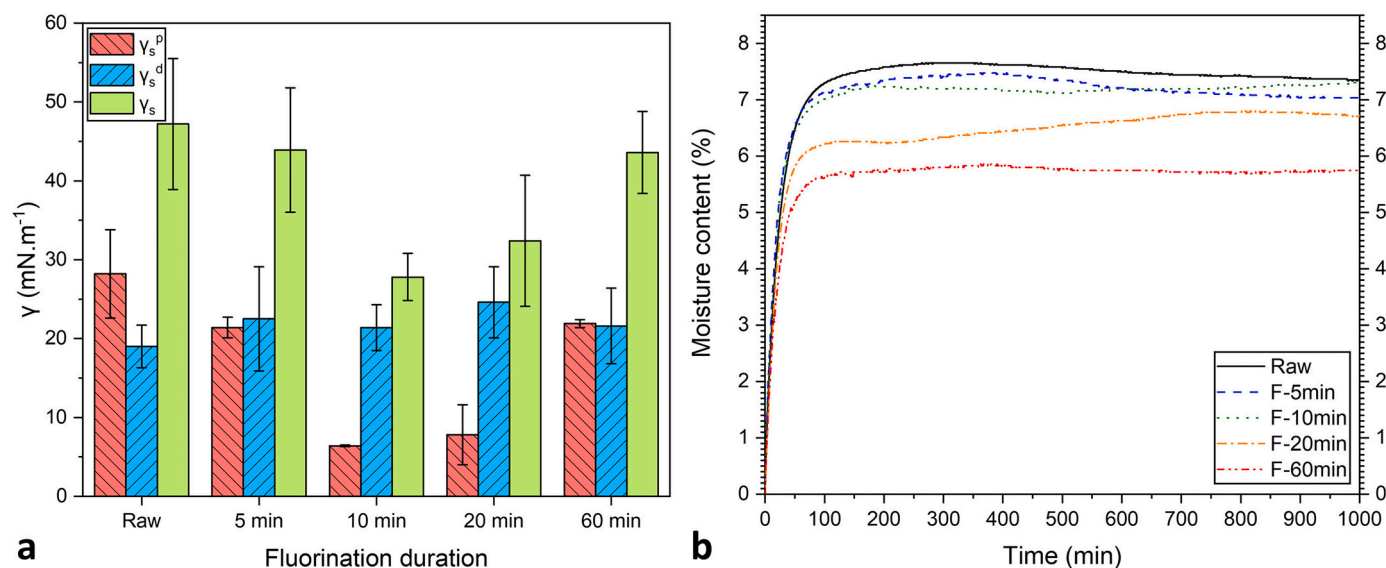
Fig. 7. a) Polar, dispersive and total surface energy of fluorinated flax fibers; b) Dynamic Vapor Sorption of untreated and fluorinated flax fibers (Area 3) at fixed relative humidity: 60%.

Table 5), for completion of the decrease of γ_s^p. On the other hand, after 10 min of fluorination, although the surface composition of the sample is approximately the same than for F-5 min (data from XPS), its composition in the whole fluorinated layer is strongly modified, as shown in the FT-IR spectra (Fig. 3). Indeed, between samples F-5 min and F-10 min, a clear increase in the contribution of the C—F bonds is observed for the more fluorinated sample, indicating that the fluorinated layer is thicker after 10 min of treatment and explaining the weaker polarity of F-10 min sample. At 20 min of fluorination if, on the one hand, the grafted fluorine quantity is higher than after 10 min (Table 4), degradation of fibers has begun, as observed in FTIR spectra (Fig. 3), and coherent with Fig. 7a, by comparing error bars for F-10 min and F-20 min samples. Indeed, F-10 min present a very low standard deviation (0.1 mN/m) when compared to the F-20 min sample. This phenomenon is due to the degradation in F_2 gas that generates disparity between areas, and consequently, shows more variable results. When further considering the uncertainties, it is evident that the F-10 min sample is more homogeneous than the F-5 min itself, which is much more homogeneous than the raw one; vegetal fibers are natural materials, which present a great disparity between them [10]. When it is well controlled, fluorination treatment allows this variability to be limited and a surface energy with a reduced dispersion is obtained for treated fibers compared to the raw ones. From an industrial point of view, this appears as extremely interesting and promising. Standard deviation of F-60 min sample is pretty small (0.4 nM/m), evidencing that this degradation is uniformly distributed onto the fibers.

Moreover, the dispersive component remains nearly constant for fluorinated samples, after a very slight increase, i.e. from 19.0 to 22.5 mN/m for raw and F-5 min sample, respectively. Then fluorination does not affect significantly the dispersive component for flax fibers, contrarily to the case of polymers [52,92]. However, Pouzet et al. [49] have also found a stability of the γ_s^d for wood after short fluorination time. This component started to increase for longer fluorination times, when the degradation started to appear. Thereby, and knowing the fact that the dispersive constant is strongly related to the surface texture [45], surface modification highlighted by the standard deviation must be at a very small scale to not affect more significantly the dispersive component.

3.2.2. Modification of the water sorption

Another point of interest for composite is the reduction of the water

sorption for applications in aquatic areas (boat for example) or in places where they will be subject to water sorption (rainy region, seaside, etc.). Fig. 7b displays the equivalent DVS profiles of flax fibers at 60% of relative humidity. However, relative humidity is fixed using saturated salt solution and ambient temperature affects the RH% value. Thereby, slight fluctuations are observed on DVS curves because of these temperature variations. Results showed that water sorption is significantly reduced thanks to the fluorination treatment. For 5 and 10 min, a slight decrease is observable, but because of the uncertainties due to temperature variation, it is not possible to firmly conclude. However, for 20 and 60 min, fluorination allows clearly the water sorption of fibers to be decreased. Consequently, significantly fluorinated fibers reduces the fibers water sorption and thus, avoids potential swelling of the fibers, which could generate cracks into the composite and thus greatly alter its mechanical performance [14].

The presence of C—F groups in substitution of C—OH explains the decrease of the adsorption of water molecules on the fibers surface. This phenomenon is evidenced by the water contact angles value of the fibers (presented in Supporting Information, Fig. SI.1). If the angle value as such has no scientific significance because it is distorted by the texture effects and size of the fibers, the increase of 20° between the raw fibers and those fluorinated 10 min demonstrates the hydrophobicity enhancement of the latter. In addition, the external fibers walls are the "entrance doors" to the fiber cells. Regions where the lignin content is the highest, that is, middle lamella and primary cell, will consume fluorine gas first and fix fluorine atoms. This may localize the covalent grafting of fluorine atoms mainly in those parts. In the mild fluorination conditions in terms of duration fluorine quantity CHF, CF_2, and CF_3 groups are mainly located in the outer parts of the cell maintaining the inner ones non-modified. Therefore, the fluorination allows to limit both types of sorption: in the volume (absorption) and on the surface (adsorption), which necessarily reduces the water content of the fibers (and the more fluorine there is, the more this water content is reduced).

3.2.3. Morphological changes

As mentioned earlier, fluorination may act on surface roughness of treated fibers via the decomposition in a process, similar to a chemical etching [45,52,81]. If a weak surface roughness of fibers is beneficial for composite manufacturing by creating a possibility of mechanical anchoring between the reinforcement and the matrix and consequently an improvement the mechanical properties of the final composite, high

surface roughness can be detrimental because it decreases the wettability by the polymer matrix. Thereby, to observe and quantify this phenomenon, SEM analyses (Fig. 8) and AFM experiments (Fig. 9) were carried out. For the AFM pictures, indication of position will be made using coordinates that correspond to the ones present on each images of the Fig. 9, and the orientation of the x,y,z axes is indicated on the left bottom hand corner and follow the right-hand rule. Coordinates will be written as following (X value; Y value).

Whether the treatment duration time, no significant modification appears on SEM pictures (2000× of magnification). On the contrary, the overfluorinated sample exhibits a very strong degradation in accordance with the surface energy. A nanometric scale is needed to evidence the roughness changes with the fluorination treatment. Raw fibers exhibit a high surface roughness with Ra of 42.2 nm and Rq of 61.6 nm with flat areas surrounded by more uneven areas (Fig. 9, raw label), at the coordinates (x;y) (1;1.5) and (1;0.5) respectively. After fluorination for 10 min, a decrease of the surface roughness is recorded (Ra = 13 and Rq = 19.1 nm). However, if flat area (Fig. 9, F-10 min label) (1;1) and uneven areas (1.5;2), are still present, picture evidences a beginning of surface etching, with the appearance of small bulbs at the fiber surface. For 60 min of fluorination, once again, formerly flat area (Fig. 9, F-60 min label) (1;1) and uneven areas are still remaining (0.5;1) and (2;1), but are scattered with much more important and visible etching points on the surface. However, for "flat" areas, etching seems, visually, less pronounced than uneven areas. This could indicate that fluorine preferentially react on bumps areas and tends to balance the average height of the surface while creating a roughness (as already observed in other works [51,52]). This etching increases the value of the surface roughness in comparison with 10 min of fluorination (Ra = 31.3 and Rq = 41.2 nm).

It is well known that the chemical etching may increase the hydrophobic character through the decrease of the polar component, because of fakir effect. However, as observed on Fig. 7a, this case is not reached for the F-60 min sample because of the nanoscale of the rugosity.

3.2.4. Mechanical properties

Considering the chemical change at the fibers surface, mechanical change may be also observed due to the fluorination treatment. In order to check that, tensile tests were performed, and the data are presented in Fig. 10. The high experimental error bars (up to 50%) are due to the variability of natural fibers and not related to the method employed to measure tensile properties of flax fibers; experimental uncertainties being of the order of 5%, significantly lower than the standard deviations with is up to 50% [52].

The tensile tests evidence that the Young's modulus (Fig. 10a) is still constant with the increase of the fluorination duration. On the contrary, both ultimate tensile strength and maximum of elongation decrease with increasing fluorination duration. This is explained by the fact that fluorination only affects the outmost surface of the fibers. However, Young's modulus reflects volume properties of the material while ultimate tensile strength and maximum of elongation are more related to surface properties. Thereby, surface modification and defaults generated by the fluorination treatment on the fiber surface allow the properties at rupture to be decreased, e.g. ultimate tensile strength and maximum of elongation (the reason why Young's modulus remains constant is described in more details in the Supporting Information). However, Liotier et al. [34] have already demonstrate that, even if fiber properties at rupture are reduced by a given treatment (thermal treatment in their case), if this treatment allows to improve wettability of fibers with the polymer matrix, the overall mechanical behavior of composites manufactured is improved with treated fibers. Then, this decrease of strength is probably not a problem in view of the intended application in composite manufacturing.

Thereby, in terms of fluorination impact, it can be stated that the treatment significantly reduces the fiber polarity as well as their capacity to water sorption. In addition, an optimum of polarity reduction was found (10 min in our case) whereas the water sorption reduction is continuous with the treatment duration. The degradation at the nanometric scale, evidenced by AFM contrary to SEM (x2000), induces damage in the mechanical properties at break, i.e. σ_m and A% (which remains moderate). On the other hand, as the treatment is localized on the outmost surface and does not affect the cellulose but only the lignin, Young's modulus remains unchanged.

3.3. Fluorine release

One of the main inquiries about fluorinated compound is fluorine release during heating, because of the hazardousness of the gases release, such as HF or F_2. In order to quantify these releases, TGA coupled with MS analysis was performed on the optimum sample (F-10 min) and the sample which underwent the longest treatment (F-60 min), in order to have a global idea of the various releases which can take place according to the temperature (overfluorinated sample, unfortunately could not be analyzed because of the small amount available). These experiments allow to simultaneously acquire the weight loss by sample when the temperature increases and identify molecular
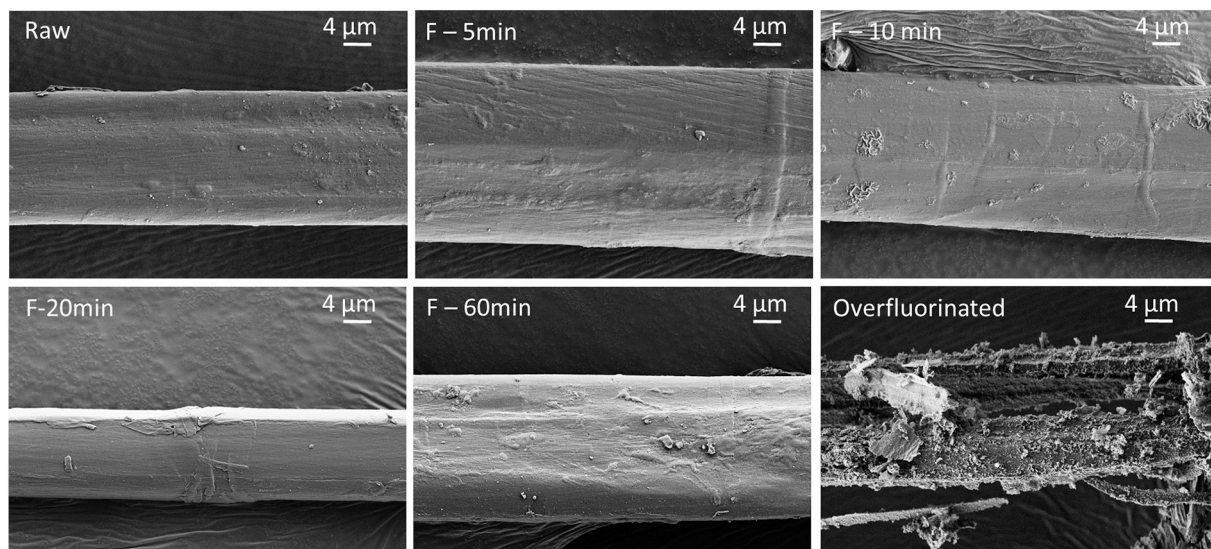

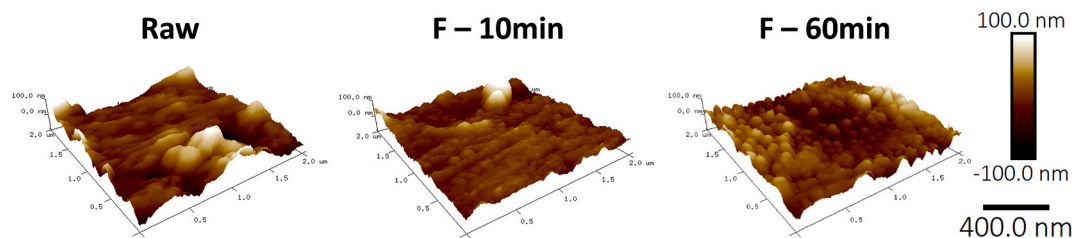**Fig. 8.** SEM pictures of raw and fluorinated flax fibers.

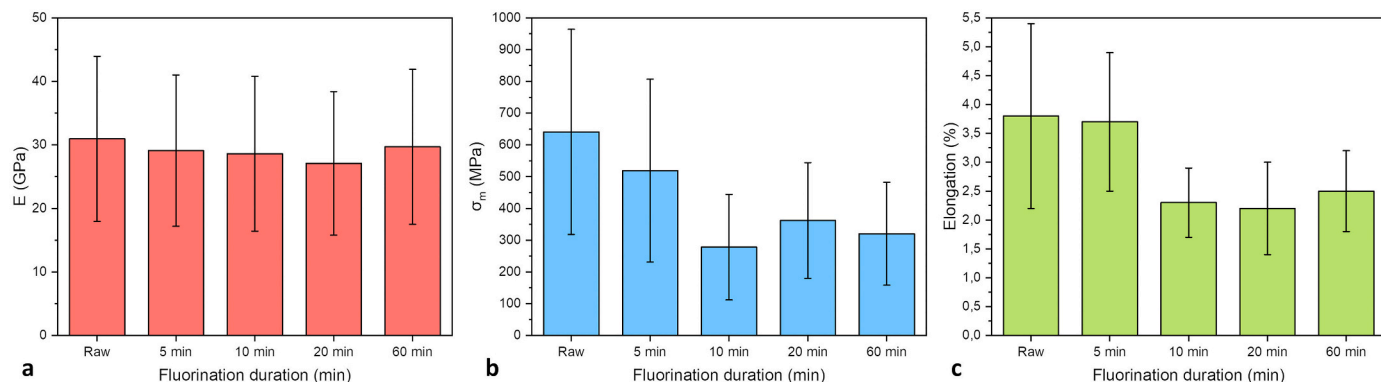**Fig. 9.** AFM images of raw and fluorinated flax fibers.

Fig. 10. Evolution of the fiber mechanical properties with the fluorination duration: (a) Young's modulus; (b) Ultimate tensile strength; (c) % of maximal elongation.

fragments, that are contained in the gases released during combustion (Fig. 11 and Fig. 12). More precisely, Fig. 11 displays the TG curves of raw and fluorinated samples (solid line) and the evolution of the intensity of two specific mass peaks, i.e. $m/Z = 19$ and 69 witch respectively correspond to F and CF_3 fragments (dash-dot-dot line and dash line on the figure, respectively). Fig. 12a shows the global mass spectrum (on the overall of the experiment) and Fig. 12b, the mass spectrum at 350 °C, temperature for which the decomposition is maximum.

First, on Fig. 12b the absence of big fragments is underlined; only the H_2O ($m/z = 18$), the CO ($m/z = 28$) and the CO_2 ($m/z = 44$) peaks (and their isotopic abundance homologues) may be observed. This evidences that C—F bonds are broken rather than the departure of large gas fragments (CF_4, C_2F_6, etc.). Hence the study of the fragments with $m/z = 19$ (F) and 69 (CF_3) in Fig. 11 for sample fluorinated during 10 and 60 min clearly reveals that CF_3 is released in very small amount, and only at

350 °C (their quantity is so small that it is almost anecdotal). F is released in higher quantity than CF_3. Before 100 °C, no trace of fluorine has been detected. Then, between 100° and 250° a small increase before a stabilization of the F quantity detected are observed. This amount of fluorine is related to F atom physiorbed on the surface of flax fibers. Then, the quick increase in the amount of fluorine released is related to the thermal breaking of C—F bonds, with a maximum of release at 350 °C. At this temperature, most of the removable fluorine is released and the amount of fluorine evolved decreases abruptly to 0; the quantity observed after 600 °C is due to the remanence of fluorine typical for m/z = 19.

3.4. Comparison of fluorination and torrefaction

Torrefaction treatment is frequently used at industrial scale to reduce the polar character of vegetal fibers by destroying hemicelluloses, the most polar component of lignocellulosic materials. Thereby, we have compared the diminution of the polarity of flax fiber with a conventional torrefaction treatment (230 °C-30 min) and our optimum fluorination treatment (10 min fluorination). Results (Fig. 13) evidence that, under the chosen conditions of the torrefaction treatment according to the optimized torrefaction to improve fiber/matrix adhesion in a biocomposite performed by Berthet et al. [22], fluorination decreases the polarity of the fibers much more significantly than torrefaction. The values are of 6.4 ± 0.1 mN/m and 19.8 ± 8.2 mN/m, respectively.

In view of this result, combination of torrefaction and fluorination appeared as a promising route to further reduce the polar character of flax fibers (surface and bulk), as already realized by Pouzet et al. on wood samples [93]. However, if the covalent grafting of fluorine was successful on torrefied fibers (Fig. 14 showing XPS data), wetting tests (Table 6) do not evidence a reduction of the polarity of fibers as expected; on the contrary, the longer the fluorination treatment, the higher the polar component of surface tension. Any of the fluorination conditions results in an enhancement for given torrefaction conditions.

The degradation resulting from the torrefaction is not compatible with the fluorination. Indeed, at 230 °C, lignin and cellulose are degraded, and with fluorination treatment, the already weakened fibers
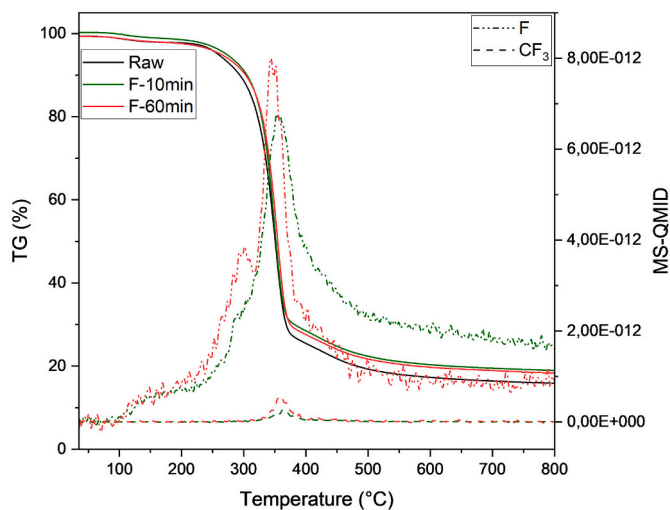

Fig. 11. ATG-MS curves for raw and fluorinated samples (F-10 min and F-60 min).
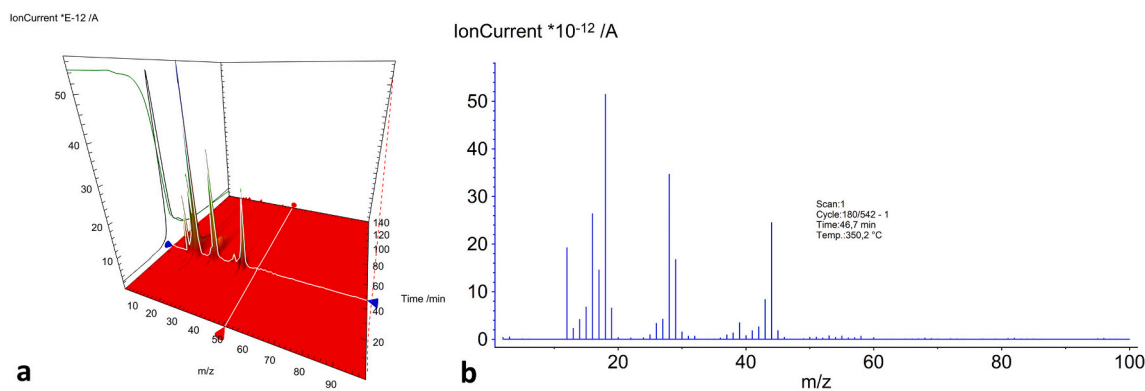
Fig. 12. Global mass spectrum a) on the overall experience of the experiment b) at 350 °C (maximum of decomposition).
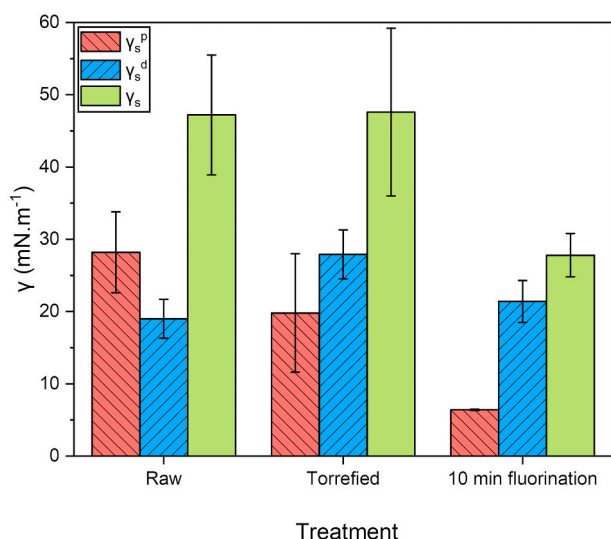

Fig. 13. Comparison of the torrefaction treatment and the fluorination treatment effects on polar, dispersive and total surface energy.

have been further damaged by the treatment, which would explain the increase of the fiber polarity. Milder conditions of torrefaction combined with fluorination would be investigated before to conclude about the efficiency of torrefaction/fluorination for eco-composite manufacturing.

4. Conclusion

Direct fluorination in static condition with molecular fluorine gas F_2 was performed on flax fibers substrate. This treatment allows fluorine atoms to be contently grafted at the outmost surface of these fibers, even after a short treatment duration (5 min). The FT-IR, ^{19}F NMR and XPS analyses have allowed to better understand the fluorination mechanism on flax fibers evidencing the conversion of COH and C—H into C—F bonds.

Thanks to this treatment, flax fibers polarity has been decreased from 19.0 mN/m to 6.4 mN/m(for 10 min of fluorination), and consequently this material has a much better compatibility with mostly dispersive polymer matrix, e.g. polypropylene, epoxy, etc. Because fluorination only affects the outmost surface of fibers, bulk properties (like young modulus) are maintained.

It has been also tried to combine torrefaction and fluorination treatments in order to further improved the dispersive character of flax fibers. However, in this case, the treatment did not produce the expected results. Nevertheless, by comparing the diminishing of the polarity obtained with the torrefaction treatment, and with the fluorination, the higher efficiency of fluorination alone is demonstrated. Most of the technological barriers were overcome: i) no release of toxic fluorinated species during burning, ii) a minute control of the fluorination

Table 6
Polar, dispersive and total surface energy of torrefied-fluorinated flax fibers.

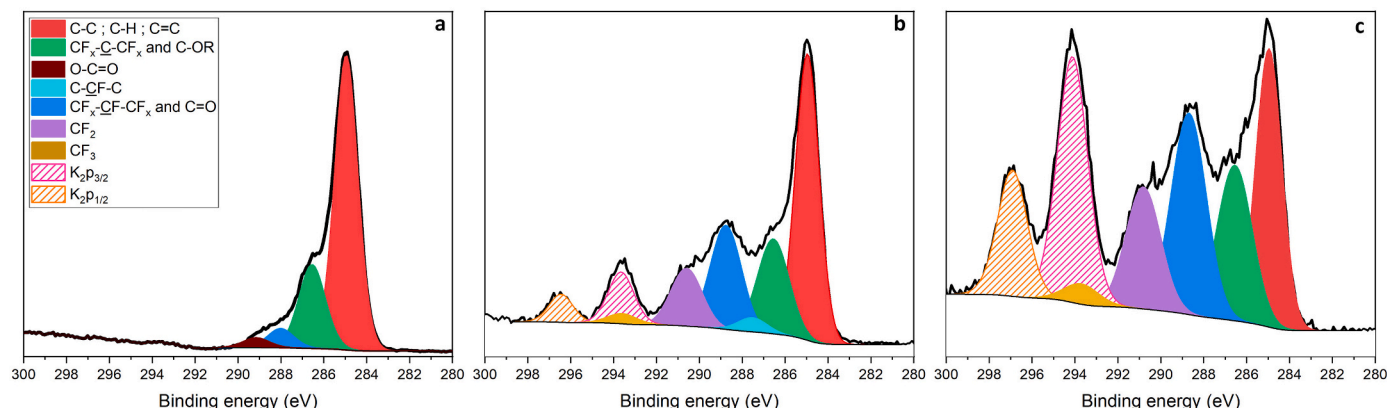| Sample	γ_s^p (mN/m)	γ_s^d (mN/m)	γ_s^{tot} (mN/m)
Raw	28.2 ± 5.5	19.0 ± 2.7	47.2 ± 8.3
Torrefied	19.8 ± 8.2	27.9 ± 3.4	47.6 ± 11.6
Torrefied +5 min fluorination	34.0 ± 1.0	20.7 ± 5.0	54.7 ± 6.9
Torrefied +10 min fluorination	28.2 ± 13.4	24.2 ± 2.7	52.4 ± 16.0
Torrefied +20 min fluorination	34.7 ± 4.5	25.9 ± 4.2	61.7 ± 8.6
Torrefied +60 min fluorination	38.2 ± 5.7	25.7 ± 4.4	63.8 ± 10.0

Fig. 14. C1s XPS spectra of flax fibers (a) torrefied, (b) torrefied-fluorinated (10 min), (c) torrefied-fluorinated (60-min).

conditions allows the chemical etching to be negligible in comparison with the benefits. The scale-up of the treatment is under progress with the aim to avoid the burning of some parts close to the reactive gas injection while keeping the same advantages.

CRediT authorship contribution statement

Olivier Téraube: Conceptualization, Methodology, Software, Validation, Formal analysis, Investigation, Data curation, Writing – original draft, Visualization. **Jean-Charles Agopian:** Formal analysis, Investigation, Writing – review & editing. **Monica Francesca Pucci:** Methodology, Validation, Resources, Writing – review & editing. **Pierre-Jacques Liotier:** Methodology, Validation, Resources, Writing – review & editing. **Samar Hajjar-Garreau:** Investigation, Resources, Writing – review & editing. **Nicolas Batisse:** Investigation, Validation, Resources, Writing – review & editing. **Karine Charlet:** Conceptualization, Methodology, Resources, Writing – review & editing, Supervision, Project administration. **Marc Dubois:** Conceptualization, Methodology, Resources, Writing – review & editing, Supervision, Project administration, Funding acquisition.

Declaration of Competing Interest

The authors declare that they have no known competing financial interests or personal relationships that could have appeared to influence the work reported in this paper.

Acknowledgment

Appendix A. Supplementary data

Supplementary data to this article can be found online at https://doi.org/10.1016/j.susmat.2022.e00467.

References

[1] J.S. Dhaliwal, Natural fibers: applications, in: M. Abbas, H.-Y. Jeon (Eds.), Generation, Development and Modifications of Natural Fibers, IntechOpen, 2019, https://doi.org/10.5772/intechopen.86884.

[2] K. Charlet, Contribution à l'étude de composites unidirectionnels renforcés par des fibres de lin: relation entre la microstructure de la fibre et ses propriétés mécaniques, Thèse en chimie des matériaux, Université de Caen, 2006.

[3] A. Moudood, A. Rahman, A. Öchsner, M. Islam, G. Francucci, Flax fiber and its composites: an overview of water and moisture absorption impact on their performance, J. Reinf. Plast. Compos. 38 (2019) 323–339, https://doi.org/10.1177/0731684418818893.

[4] J. Holbery, D. Houston, Natural-fiber-reinforced polymer composites in automotive applications, JOM 58 (2006) 80–86, https://doi.org/10.1007/s11837-006-0234-2.

[5] C.-M. Wu, W.-Y. Lai, C.-Y. Wang, Effects of surface modification on the mechanical properties of flax/β-polypropylene composites, Materials 9 (2016) 314–324, https://doi.org/10.3390/ma9050314.

[6] F.M. AL-Oqla, M.S. Salit, Natural fiber composites, in: Materials Selection for Natural Fiber Composites, Elsevier, 2017, pp. 23–48.

[7] M. Asim, K. Abdan, M. Jawaid, M. Nasir, Z. Dashtizadeh, M.R. Ishak, et al., A review on pineapple leaves fibre and its composites, Int. J. Polym. Sci. 2015 (2015) 1–16, https://doi.org/10.1155/2015/950567.

[8] P. Wambua, J. Ivens, I. Verpoest, Natural fibres: can they replace glass in fibre reinforced plastics? Compos. Sci. Technol. 63 (2003) 1259–1264, https://doi.org/10.1016/S0266-3538(03)00096-4.

[9] L. Yan, N. Chouw, K. Jayaraman, Flax fibre and its composites – a review, Compos. Part B 56 (2014) 296–317, https://doi.org/10.1016/j.compositesb.2013.08.014.

[10] K. Charlet, C. Baley, C. Morvan, J.P. Jernot, M. Gomina, J. Bréard, Characteristics of Hermès flax fibres as a function of their location in the stem and properties of the derived unidirectional composites, Compos Part A: Appl Sci Manuf 38 (2007) 1912–1921, https://doi.org/10.1016/j.compositesa.2007.03.006.

[11] K. Charlet, J.-P. Jernot, M. Gomina, L. Bizet, J. Bréard, Mechanical properties of flax fibers and of the derived unidirectional composites, J. Compos. Mater. 44 (2010) 2887–2896, https://doi.org/10.1177/0021998310369579.

[12] C. Baley, A. Bourmaud, Average tensile properties of French elementary flax fibers, Mater. Lett. 122 (2014) 159–161, https://doi.org/10.1016/j.matlet.2014.02.030.

[13] M.F. Pucci, P.-J. Liotier, D. Seveno, C. Fuentes, A. Van Vuure, S. Drapier, Wetting and swelling property modifications of elementary flax fibres and their effects on the Liquid Composite Molding process, Compos Part A: Appl Sci Manuf 97 (2017) 31–40, https://doi.org/10.1016/j.compositesa.2017.02.028.

[14] H. Dhakal, Z. Zhang, M. Richardson, Effect of water absorption on the mechanical properties of hemp fibre reinforced unsaturated polyester composites, Compos. Sci. Technol. 67 (2007) 1674–1683, https://doi.org/10.1016/j.compscitech.2006.06.019.

[15] L. Chotirat, K. Chaochanchaikul, N. Sombatsompop, On adhesion mechanisms and interfacial strength in acrylonitrile–butadiene–styrene/wood sawdust composites, Int. J. Adhes. Adhes. 27 (2007) 669–678, https://doi.org/10.1016/j.ijadhadh.2007.02.001.

[16] M. Kazayawoko, J.J. Balatinecz, L.M. Matuana, Surface modification and adhesion mechanisms in woodfiber-polypropylene composites, J. Mater. Sci. (1999) 6189–6199.

[17] C. Klason, J. Kubát, H.-E. Strömvall, The efficiency of cellulosic fillers in common thermoplastics. Part 1. Filling without processing aids or coupling agents, Int. J. Polym. Mat. Po. 10 (1984) 159–187, https://doi.org/10.1080/00914038408080268.

[18] A. Célino, S. Fréour, F. Jacquemin, P. Casari, The hygroscopic behavior of plant fibers: a review, Front. Chem. 1 (2014) 1–12, https://doi.org/10.3389/fchem.2013.00043.

[19] V.K. Thakur, M. Thakur, M.R. Kessler, Handbook of Composites from Renewable Materials vol. 4, Scrivener Publishing LLC, 2017.

[20] A.J. Stamm, H.K. Burr, A.A. Kline, Staybwood—heat-stabilized wood, Ind. Eng. Chem. 38 (1946) 630–634, https://doi.org/10.1021/ie50438a027.

[21] F. Mburu, S. Dumarçay, J.F. Bocquet, M. Petrissans, P. Gérardin, Effect of chemical modifications caused by heat treatment on mechanical properties of Grevillea robusta wood, Polym. Degrad. Stab. 93 (2008) 401–405.

[22] M.-A. Berthet, J.-M. Commandré, X. Rouau, N. Gontard, H. Angellier-Coussy, Torrefaction treatment of lignocellulosic fibres for improving fibre/matrix adhesion in a biocomposite, Mater. Des. 92 (2016) 223–232, https://doi.org/10.1016/j.matdes.2015.12.034.

[23] L. Podgorski, B. Chevet, L. Onic, Modification of wood wettability by plasma and corona treatments, Int. J. Adhes. Adhes. (2000) 103–111, https://doi.org/10.1016/S0143-7496(99)00043-3.

[24] C. Lux, Z. Szalay, W. Beikircher, D. Kováčik, H.K. Pulker, Investigation of the plasma effects on wood after activation by diffuse coplanar surface barrier discharge, Eur. J. Wood Prod. 71 (2013) 539–549, https://doi.org/10.1007/s00107-013-0706-3.

[25] A. Ashori, M. Babaee, M. Jonoobi, Y. Hamzeh, Solvent-free acetylation of cellulose nanofibers for improving compatibility and dispersion, Carbohydr. Polym. 102 (2014) 369–375, https://doi.org/10.1016/j.carbpol.2013.11.067.

[26] M.J.A. Chowdhury, P.E. Humphrey, The effect of acetylation on the shear strength development kinetics of phenolic resin-to-wood bonds, Wood Fiber Sci. 31 (1999) 293–299.

[27] M. Jonoobi, J. Harun, A.P. Mathew, M.Z.B. Hussein, K. Oksman, Preparation of cellulose nanofibers with hydrophobic surface characteristics, Cellulose 17 (2010) 299–307, https://doi.org/10.1007/s10570-009-9387-9.

[28] V. Tserki, N.E. Zafeiropoulos, F. Simon, C. Panayiotou, A study of the effect of acetylation and propionylation surface treatments on natural fibres, Compos Part A: Appl Sci Manuf 36 (2005) 1110–1118, https://doi.org/10.1016/j.compositesa.2005.01.004.

[29] J.A. Youngquist, R.M. Rowell, Dimensional stability of acetylated Aspen Flakeboard, Wood Fiber Sci. 18 (1986) 90–98.

[30] M. Kazayawoko, J.J. Balatinecz, R.T. Woodhams, R.N.S. Sodhi, X-ray photoelectron spectroscopy of lignocellulosic materials treated with Malea ted polypropylenes, J. Wood Chem. Technol. 18 (1998) 1–26, https://doi.org/10.1080/02773819809350122.

[31] B. Mohebby, P. Fallah-Moghadam, A.R. Ghotbifar, S. Kazemi-Najafi, Influence of maleic-anhydride-polypropylene (MAPP) on wettability of polypropylene/wood flour/glass Fiber hybrid composites, J. Agric. Sci. Technol. 13 (2011) 877–884.

[32] S. Phillips, J. Baets, L. Lessard, P. Hubert, I. Verpoest, Characterization of flax/epoxy prepregs before and after cure, J. Reinf. Plast. Compos. 32 (2013) 777–785, https://doi.org/10.1177/0731684412473359.

[33] C. Tang, M. Wu, Y. Wu, H. Liu, Effects of fiber surface chemistry and size on the structure and properties of poly(vinyl alcohol) composite films reinforced with electrospun fibers, Compos. A: Appl. Sci. Manuf. 42 (2011) 1100–1109, https://doi.org/10.1016/j.compositesa.2011.04.015.

[34] P.-J. Liotier, M.F. Pucci, A. Le Duigou, A. Kervoelen, J. Tirilló, F. Sarasini, et al., Role of interface formation versus fibres properties in the mechanical behaviour of bio-based composites manufactured by Liquid Composite Molding processes, Compos. Part B 163 (2019) 86–95, https://doi.org/10.1016/j.compositesb.2018.10.103.

[35] A. Dong, X. Fan, Q. Wang, Y. Yu, A. Cavaco-Paulo, Hydrophobic surface functionalization of lignocellulosic jute fabrics by enzymatic grafting of octadecylamine, Int. J. Biol. Macromol. 79 (2015) 353–362, https://doi.org/10.1016/j.ijbiomac.2015.05.007.

[36] A. Dong, Y. Yu, J. Yuan, Q. Wang, X. Fan, Hydrophobic modification of jute fiber used for composite reinforcement via laccase-mediated grafting, Appl. Surf. Sci. 301 (2014) 418–427, https://doi.org/10.1016/j.apsusc.2014.02.092.

[37] V. Fiore, T. Scalici, F. Nicoletti, G. Vitale, M. Prestipino, A. Valenza, A new eco-friendly chemical treatment of natural fibres: effect of sodium bicarbonate on properties of sisal fibre and its epoxy composites, Compos. Part B 85 (2016) 150–160, https://doi.org/10.1016/j.compositesb.2015.09.028.

[38] D. Gulati, M. Sain, Fungal-modification of natural fibers: a novel method of treating natural fibers for composite reinforcement, J. Polym. Environ. 14 (2006) 347–352, https://doi.org/10.1007/s10924-006-0030-7.

[39] X. Huang, A. Wang, X. Xu, H. Liu, S. Shang, Enhancement of hydrophobic properties of cellulose fibers via grafting with polymeric Epoxidized soybean oil, ACS Sustain. Chem. Eng. 5 (2017) 1619–1627, https://doi.org/10.1021/acssuschemeng.6b02359.

[40] T. Kick, T. Grethe, B. Mahltig, A natural based method for hydrophobic treatment of natural Fiber material, ACSi 64 (2017) 373–380, https://doi.org/10.17344/acsi.2017.3232.

[41] K. Lee, J.S. Jur, D.H. Kim, G.N. Parsons, Mechanisms for hydrophilic/hydrophobic wetting transitions on cellulose cotton fibers coated using Al$_2$O$_3$ atomic layer deposition, J. Vac. Sci. Technol. A 30 (2012) 01A163, https://doi.org/10.1116/1.3671942.

[42] K. Thakur, S. Kalia, D. Pathania, A. Kumar, N. Sharma, C.L. Schauer, Surface functionalization of lignin constituent of coconut fibers via laccase-catalyzed biografting for development of antibacterial and hydrophobic properties, J. Clean. Prod. 113 (2016) 176–182, https://doi.org/10.1016/j.jclepro.2015.11.048.

[43] Q. Wang, S. Xiao, S.Q. Shi, S. Xu, L. Cai, Self-bonded natural fiber product with high hydrophobic and EMI shielding performance via magnetron sputtering Cu film, Appl. Surf. Sci. 475 (2019) 947–952, https://doi.org/10.1016/j.apsusc.2019.01.059.

[44] A.P. Kharitonov, Practical applications of the direct fluorination of polymers, J. Fluor. Chem. 103 (2000) 123–127, https://doi.org/10.1016/S0022-1139(99)00312-7.

[45] A.P. Kharitonov, G.V. Simbirtseva, A. Tressaud, E. Durand, C. Labrugère, M. Dubois, Comparison of the surface modifications of polymers induced by direct fluorination and rf-plasma using fluorinated gases, J. Fluor. Chem. 165 (2014) 49–60, https://doi.org/10.1016/j.jfluchem.2014.05.002.

[46] A.P. Kharitonov, R. Taege, G. Ferrier, V.V. Teplyakov, D.A. Syrtsova, G.-H. Koops, Direct fluorination—useful tool to enhance commercial properties of polymer articles, J. Fluor. Chem. 126 (2005) 251–263, https://doi.org/10.1016/j.jfluchem.2005.01.016.

[47] J. Maity, C. Jacob, C.K. Das, R.P. Singh, Direct fluorination of Twaron fiber and investigation of mechanical thermal and morphological properties of high density polyethylene and Twaron fiber composites, J. Appl. Polym. Sci. 107 (2008) 3739–3749, https://doi.org/10.1002/app.27510.

[48] A.P. Kharitonov, Direct Fluorination of Polymers, Nova Publishers, 2008.

[49] M. Pouzet, M. Dubois, K. Charlet, A. Béakou, From hydrophilic to hydrophobic wood using direct fluorination: a localized treatment, C R Chim 21 (2018) 800–807, https://doi.org/10.1016/j.crci.2018.03.009.

[50] A.P. Kharitonov, L.N. Kharitonova, Surface modification of polymers by direct fluorination: a convenient approach to improve commercial properties of polymeric articles, Pure Appl. Chem. 81 (2009) 451–471, https://doi.org/10.1351/PAC-CON-08-06-02.

[51] J.-C. Agopian, O. Teraube, M. Dubois, K. Charlet, Fluorination of carbon fibre sizing without mechanical or chemical loss of the fibre, Appl. Surf. Sci. 534 (2020), 147647, https://doi.org/10.1016/j.apsusc.2020.147647.

[52] O. Teraube, J.-C. Agopian, E. Petit, F. Metz, N. Batisse, K. Charlet, et al., Surface modification of sized vegetal fibers through direct fluorination for eco-composites, J. Fluor. Chem. 238 (2020), 109618, https://doi.org/10.1016/j.jfluchem.2020.109618.

[53] Tooran Khazraie Shoulaifar, Chemical Changes in Biomass during Torrefaction, Thèse, Åbo Akademi University, 2016.

[54] J. Shankar Tumuluru, S. Sokhansanj, J.R. Hess, C.T. Wright, R.D. Boardman, A review on biomass torrefaction process and product properties for energy applications, Ind. Biotechnol. 7 (2011) 384–401, https://doi.org/10.1089/ind.2011.7.384.

[55] P.J. Van Soest, Use of detergents in the analysis of fibrous feeds. II. A rapid method for the determination of Fiber and lignin, J. Assoc. Agric. Chem. 46 (1963) 829–835.

[56] V. Dhyani, T. Bhaskar, Pyrolysis of Biomass. Biofuels: Alternative Feedstocks and Conversion Processes for the Production of Liquid and Gaseous Biofuels, 2nd ed., Elsevier, 2019, pp. 217–244.

[57] T. Young, An essay on the cohesion of fluids, Philos. Trans. R. Soc. Lond. 95 (1805) 65–87.

[58] S.L. Schellbach, S.N. Monteiro, J.W. Drelich, A novel method for contact angle measurements on natural fibers, Mater. Lett. 164 (2016) 599–604, https://doi.org/10.1016/j.matlet.2015.11.039.

[59] S. Qiu, C.A. Fuentes, D. Zhang, A.W. Van Vuure, D. Seveno, Wettability of a single carbon Fiber, Langmuir 32 (2016) 9697–9705.

[60] A. Hodzic, Z.H. Stachurski, Droplet on a fibre: surface tension and geometry, Composite Interfaces 8 (2001) 415–425, https://doi.org/10.1163/156855401753424451.

[61] J.M. Van Hazendonk, J.C. Van der Putten, J.T.F. Keurentjes, A. Prins, A simple experimental method for the measurement of the surface tension of cellulosic fibres and its relation with chemical composition, Colloids Surf. A Physicochem. Eng. Asp. 81 (1993) 251–261.

[62] D.K. Owens, R.C. Wendt, Estimation of the surface free energy of polymers, J. Appl. Polym. Sci. 13 (1969) 1741–1747, https://doi.org/10.1002/app.1969.070130815.

[63] M.F. Pucci, P.-J. Liotier, S. Drapier, Tensiometric method to reliably assess wetting properties of single fibers with resins: validation on cellulosic reinforcements for composites, Colloids Surf. A Physicochem. Eng. Asp. 512 (2017) 26–33, https://doi.org/10.1016/j.colsurfa.2016.09.047.

[64] ISO 483:2005 Plastics, Small enclosures for conditioning and testing using aqueous solutions to maintain the humidity at a constant value, 2006.

[65] A. Roudier, K. Charlet, F. Moreno, E. Toussaint, C. Géneau-Sbartaï, S. Commereuc, et al., Caractérisation des propriétés biochimiques et hygroscopiques d'une fibre de lin, Mater. Technol. 100 (2012) 525–535, https://doi.org/10.1051/mattech/2012044.

[66] NF T25-501-2 Mars 2015, Fibres de renfort - Fibres de lin pour composites plastiques - Partie 2: détermination des propriétés en traction des fibres élémentaires, 2015.

[67] G. Socrates, Infrared and Raman Characteristic Group Frequencies: Tables and Charts, 3rd ed., Wiley, Chichester; New York, 2001.

[68] A.P. Kharitonov, R. Taege, G. Ferrier, N.P. Piven, The kinetics and mechanism of the direct fluorination of polyethylenes, Surf. Coatings Int. Part B: Coatings Trans. 88 (2005) 201–212, https://doi.org/10.1007/BF02699574.

[69] M. Pouzet, M. Dubois, K. Charlet, A. Béakou, The effect of lignin on the reactivity of natural fibres towards molecular fluorine, Mater. Des. 120 (2017) 66–74, https://doi.org/10.1016/j.matdes.2017.01.086.

[70] K. Charlet, F. Saulnier, D. Gautier, M. Pouzet, M. Dubois, A. Béakou, Fluorination as an effective way to reduce natural fibers hydrophilicity, in: R. Fangueiro, S. Rana (Eds.), Natural Fibres: Advances in Science and Technology Towards Industrial Applications vol. 12, Springer Netherlands, Dordrecht, 2016, pp. 211–229, https://doi.org/10.1007/978-94-017-7515-1_16.

[71] M. Pouzet, M. Dubois, K. Charlet, A. Béakou, J.-M. Leban, M. Bada, Fluorination renders the wood surface hydrophobic without any loss of physical and mechanical properties, Ind. Crop. Prod. 133 (2019) 133–141, https://doi.org/10.1016/j.indcrop.2019.02.044.

[72] R.J. Lagow, J.L. Margrave, Direct fluorination: A "new" approach to fluorine chemistry, in: S.J. Lippard (Ed.), Progress in Inorganic Chemistry vol. 26, John Wiley & Sons, Inc., Hoboken, NJ, USA, 1979, pp. 161–210.

[73] A.J. Vega, A.D. English, Multiple-pulse nuclear magnetic resonance of solid polymers. Polymer motions in crystalline and amorphous poly (tetrafluoroethylene), Macromolecules 13 (1980) 1635–1647, https://doi.org/10.1021/ma60078a051.

[74] E. Katoh, H. Sugisawa, A. Oshima, Y. Tabata, T. Seguchi, T. Yamazaki, Evidence for radiation induced crosslinking in polytetrafluoroethylene by means of high-resolution solid-state 19F high-speed MAS NMR, Radiat. Phys. Chem. 54 (1999) 165–171, https://doi.org/10.1016/S0969-806X(98)00250-3.

[75] B. Fuchs, U. Scheler, Branching and cross-linking in radiation-modified poly (tetrafluoroethylene): a solid-state NMR investigation, Macromolecules 33 (2000) 120–124, https://doi.org/10.1021/ma9914873.

[76] T.R. Dargaville, G.A. George, D.J.T. Hill, U. Scheler, A.K. Whittaker, High-speed MAS ^{19}F NMR analysis of an irradiated fluoropolymer, Macromolecules 35 (2002) 5544–5549, https://doi.org/10.1021/ma020195q.

[77] S. Sapieha, M. Verreault, J.E. Klemberg-Sapieha, E. Sacher, M.R. Wertheimer, X-ray photoelectron study of the plasma fluorination of lignocellulose, Appl. Surf. Sci. 44 (1990) 165–169.

[78] B. Ly, M.N. Belgacem, J. Bras, M.C. Brochier Salon, Grafting of cellulose by fluorine-bearing silane coupling agents, Mater. Sci. Eng. C 30 (2010) 343–347, https://doi.org/10.1016/j.msec.2009.11.009.

[79] A. Tursi, N. De Vietro, A. Beneduci, A. Milella, F. Chidichimo, F. Fracassi, et al., Low pressure plasma functionalized cellulose fiber for the remediation of petroleum hydrocarbons polluted water, J. Hazard. Mater. 373 (2019) 773–782, https://doi.org/10.1016/j.jhazmat.2019.04.022.

[80] G. Beamson, G. Briggs, High resolution XPS of organic polymers: the Scienta ESCA300 database, J. Chem. Educ. 70 (1993) A25, https://doi.org/10.1021/ed070pA25.5.

[81] L. Luo, D. Hong, L. Zhang, Z. Cheng, X. Liu, Surface modification of PBO fibers by direct fluorination and corresponding chemical reaction mechanism, Compos. Sci. Technol. 165 (2018) 106–114, https://doi.org/10.1016/j.compscitech.2018.06.014.

[82] A. Bismarck, R. Tahhan, J. Springer, A. Schulz, T.M. Klapötke, H. Zeil, et al., Influence of fluorination on the properties of carbon fibres, J. Fluor. Chem. 84 (1997) 127–134, https://doi.org/10.1016/S0022-1139(97)00029-8.

[83] Y. Chul Woo, Y. Chen, L.D. Tijing, S. Phuntsho, T. He, J.-S. Choi, et al., CF4 plasma-modified omniphobic electrospun nanofiber membrane for produced water brine treatment by membrane distillation, J. Membr. Sci. 529 (2017) 234–242, https://doi.org/10.1016/j.memsci.2017.01.063.

[84] H. Wang, Q. Yao, C. Wang, B. Fan, Q. Sun, C. Jin, et al., A simple, one-step hydrothermal approach to durable and robust superparamagnetic, superhydrophobic and electromagnetic wave-absorbing wood, Sci. Rep. 6 (2016) 35549, https://doi.org/10.1038/srep35549.

[85] B. Rousseau, H. Estrade-Szwarckopf, Photoelectron core level spectroscopy study of K- and Rb-graphite intercalation compounds –II. Clean surfaces study, Solid State Commun. 85 (1993) 793–797, https://doi.org/10.1016/0038-1098(93)90673-B.

[86] R.H. Dastur, J.G. Bhatt, Relation of potassium to fusarium wilt of flax, Nature 201 (1964) 1243–1244, https://doi.org/10.1038/2011243a0.

[87] B. Khiari, A. Ibn Ferjani, A.A. Azzaz, S. Jellali, L. Limousy, M. Jeguirim, Thermal conversion of flax shives through slow pyrolysis process: in-depth biochar characterization and future potential use, Biomass Conv. Bioref. 11 (2021) 325–337, https://doi.org/10.1007/s13399-020-00641-0.

[88] P. Kajla, A. Sharma, D.R. Sood, Flaxseed—a potential functional food source, J. Food Sci. Technol. 52 (2015) 1857–1871, https://doi.org/10.1007/s13197-014-1293-y.

[89] B.A. Bakry, O.A. Nofal, M.S. Zeidan, M. Hozayn, Potassium and zinc in relation to improve flax varieties yield and yield components as grown under Sandy soil conditions, AS 06 (2015) 152–158, https://doi.org/10.4236/as.2015.61013.

[90] A. Goyal, V. Sharma, N. Upadhyay, S. Gill, M. Sihag, Flax and flaxseed oil: an ancient medicine & modern functional food, J. Food Sci. Technol. 51 (2014) 1633–1653, https://doi.org/10.1007/s13197-013-1247-9.

[91] W.-H. Lin, R.J. Lagow, The synthesis of highly fluorinated alkylcyclohexanes for use as oxygen carriers and the 19F and 13C NMR spectra of alkylcyclohexanes, J. Fluor. Chem. 50 (1990) 345–358, https://doi.org/10.1016/S0022-1139(00)85000-9.

[92] A.P. Kharitonov, YuL Moskvin, D.A. Syrtsova, V.M. Starov, V.V. Teplyakov, Direct fluorination of the polyimide matrimid® 5218: the formation kinetics and physicochemical properties of the fluorinated layers: direct Fluorination of Matrimid® 5218, J. Appl. Polym. Sci. 92 (2004) 6–17, https://doi.org/10.1002/app.13565.

[93] M. Pouzet, M. Dubois, K. Charlet, E. Petit, A. Béakou, C. Dupont, Fluorination/Torrefaction combination to further improve the hydrophobicity of wood, Macromol. Chem. Phys. 220 (2019) 1900041, https://doi.org/10.1002/macp.201900041.